Design of a Linker for Trivalent Thrombin Inhibitors: Interaction of the Main Chain of the Linker with Thrombin‡

Zbigniew Szewczuk,§ Bernard F. Gibbs, Shi Yi Yue, Enrico Purisima, Alexander Zdanov, Miroslaw Cygler, and Yasuo Konishi*

Biotechnology Research Institute, National Research Council of Canada, 6100 Royalmount Avenue, Montreal, Quebec H4P 2R2, Canada

Received November 12, 1992; Revised Manuscript Received January 14, 1993

ABSTRACT: N^{α}-Acetyl[D-Phe^{45},Arg^{47}]hirudin$^{45-65}$ (P53) is a bivalent thrombin inhibitor (K_i = 5.6 nM) that consists of an active site inhibitor segment, [N^{α}-acetyl-(dF)PRP]; a fibrinogen recognition exo site inhibitor segment, hirudin$^{55-65}$ (DFEEIPEEYLQ-OH); and a linker, hirudin$^{49-54}$ (QSHNDG), connecting these inhibitor segments (DiMaio et al., 1990). The structure–function relationships of the linker were studied using a combination of various ω-amino acids, which modified the length of the linker as well as the number and the locations of peptide bonds. Linkers with 14–18 atoms (counting only the atoms contributing to the length of the linker) showed a competitive inhibition with K_i = 1.7–3.4 nM. The potency of the inhibitors with 12–13-atom linkers was sensitive to the chemical structure of the linker. The high-potency inhibitors showed a competitive inhibition, while the low-potency inhibitors showed a hyperbolic inhibition. Among them, an inhibitor with a 13-atom linker showed the highest potency (K_i = 0.51 nM, an 11-fold improvement from that of P53 above), indicating that this is an optimal linker length. Since linkers with 6–10 atoms failed to bridge the active site and exo site inhibitor segments, a minimum of 11 atoms was required to bridge them, even though the potency of the inhibitor with an 11-atom linker was weak (K_i = 26 nM). Molecular dynamics simulation of the inhibitors with 13-atom linkers suggested that some linkers serve as a functional domain with the amide bond of the linker interacting with thrombin through hydrogen bonds. These inhibitors may be newly classified as trivalent inhibitors rather than bivalent inhibitors.

Cardiovascular diseases account for approximately 40% of the deaths in North America. One of the most deadly effects of cardiovascular diseases is the heart attack. An acute blockage of a coronary artery by thrombus causes a heart attack. If a large artery which nourishes a large part of the heart is blocked, the attack is more likely to be fatal. However, the chances of recovery are good if the blockage occurs in one of the smaller coronary arteries. A heart attack in its early stages may be treated by injecting tissue plasminogen activator, urokinase, or streptokinase (Cheseboro et al., 1987; Verstraete et al., 1985; While et al., 1989; Wilcox et al., 1988). These enzymes activate plasminogen to plasmin, which in turn lyses the fibrin present in a coronary thrombus, thus restoring the blood flow to the heart muscle. However, their clinical application has been associated with several significant limitations, including acute thrombotic reocclusion in a high percentage of treated patients (Marder & Sherry, 1988; Topol, 1989; Verstraete, 1990). Thrombus-bound thrombin, which is still active, has been suggested to contribute to rethrombosis after thrombolytic therapy (Agnelli et al., 1991). Furthermore, it is suggested that thrombolysis treatment induces an enhanced physiological activation of the coagulation system (Munkvad et al., 1991). In contrast to plasma-free thrombin, thrombus-found thrombin is poorly accessible to heparin, a widely used anticoagulant (Hogg & Jackson, 1989; Weitz et al., 1990). Consequently, the bound thrombin remains active and favors the occurrence of rethrombosis (Agnelli et al., 1991), indicating the need for potent and specific pharmacological agents.

Many compounds have been reported to inhibit the activity of thrombin incorporated in the thrombus. Small active site directed synthetic inhibitors (Stürzebecher, 1984) such as derivatives of a tripeptide, D-Phe-Pro-Arg, having high and selective antithrombin activity (Bajusz et al., 1978; Kettner & Shaw, 1979), effectively block the clot-bound thrombin. However, one characteristic that applies to all of these active site directed synthetic inhibitors is their short half-life of less than several minutes (Badimon et al., 1991). These inhibitors may not be effective against thrombin activity that occurs as a result of the activation of the coagulation system by thrombolytic theray (Badimon et al., 1991).

Another approach to the selective inhibition of thrombin has been by the use of hirudin, a 65 amino acid anticoagulant protein produced in the salivary glands of the European medicinal leech *Hirudo medicinalis*. Hirudin binds tightly to thrombin ($K_d \approx 10^{-14}$ M, Stone and Hofsteenge (1986)), thereby inhibiting not only cleavage of fibrinogen but also factor V activation (Fenton et al., 1991a,b), which in turn prevents continual thrombin generation. The high specificity of hirudin for thrombin and the tightness of binding are due to interactions both at the active site and at a fibrinogen recognition exo site (FRE)[1] of the enzyme (Rydel et al., 1990). The C-terminal 11 amino acid fragment (residues 55–65) of hirudin binds to the FRE (Skrzypczak-Jankun et al., 1991), while the N-terminal 48 amino acid residue fragment,

‡ NRCC Publication No. 33713.

* Author to whom correspondence should be addressed.

§ Present address: Institute of Chemistry, Wroclaw University, 50-383 Wroclaw, Poland.

[1] Abbreviations: Abu, 4-aminobutyric acid; Ac, acetyl; Aca, 6-aminocaproic acid; Ada, 12-aminododecanoic acid; Aha, 7-aminoheptanoic acid; Bal, β-alanine; AMC, 7-amino-4-methylcoumarin; Boc, *tert*-butyloxycarbonyl; BOP, (benzotriazol-1-yloxy)tris(dimethylamino)phosphonium hexafluorophosphate; Bzl, benzyl; DMF, dimethylformamide; FRE, fibrinogen recognition exo site; HPLC, high-performance liquid chromatography; rms, root mean square; TFA, trifluoroacetic acid; Tos, tosyl; Tris, 2-amino-2-(hydroxymethyl)-1,3-propanediol.

0006-2960/93/0432-3396$04.00/0 Published 1993 by the American Chemical Society

especially the three N-terminal residues, blocks the catalytic active site (Rydel et al., 1991). The gaps are connected by a six-residue linker (hirudin$^{49-54}$). Besides its high specificity and tight binding, hirudin does not have acute side effects when administered subcutaneously or intravenously in antithrombin doses in humans and is a weak antigen (Badimon et al., 1991). Furthermore, hirudin has a long lifetime of 50 min when given subcutaneously or intravenously (Markwardt et al., 1984).

These advantages of hirudin motivated the design of synthetic thrombin inhibitors, which are based on the hirudin sequence, mimic the distinctive mechanism of hirudin with reduced size, and may further improve the therapeutic activity over hirudin. Typically, the bulky active site inhibitor segment, hirudin$^{1-47}$, was replaced by a small active site inhibitor segment, D-Phe-Pro-Arg (Maraganore et al., 1990; DiMaio et al., 1990; Bourdon et al., 1991). This replacement reduced the molecular mass of the inhibitors from 7000 Da of hirudin to around 2500 Da with some loss in potency. A replacement of the Arg^{47}-Pro^{48} scissile bond with a pseudo-peptide bond restored some of the lost potency (up to 0.14 nM, DiMaio et al. (1991, 1992)).[2] The FRE inhibitor segment, hirudin$^{55-65}$, which, by itself, showed the anticoagulant and antiplatelet effects of hirudin (Jakubowski & Maraganore, 1990), was also modified to enhance its potency and proteolytic stability while reducing its size. The IC_{50} of the FRE inhibitor was improved 35-fold by a multiple substitution of residues Asp^{55}, Phe^{56}, Glu^{58}, Tyr^{63}, Leu^{64}, and Gln^{65} with succinic acid, Tyr, Pro, Ala, β-cyclohexylalanine, and D-Glu, respectively (Krestenansky et al., 1990). The low proteolytic stability of the FRE inhibitor (Knadler et al., 1992) was drastically improved by side chain to side chain cyclization between Glu^{58} and a substituted Lys^{61} with 2–4-fold improvement of the IC_{50} (Szewczuk et al., 1992b). Furthermore, the size of the FRE inhibitor was reduced from 11 to 7 residues with minimum loss in potency. This modification was successfully incorporated into a bivalent inhibitor (DiMaio et al., 1992).

In the investigations cited above, attention was focused mainly on the active site and FRE inhibitor segments, and the role of the linker was limited to provide an appropriate spacing (spacer) between the two segments. Studies of structure–activity relationships of the linker indicated that none of the side chains in the linker contributed significantly to the binding and could be replaced by Gly or some other amino acids without considerably reducing the activity (Szewczuk et al., 1992a; Yue et al., 1992). This was further confirmed by a crystal structure and a molecular dynamics simulation of N^{α}-acetyl[D-Phe^{45},Argψ(CO-CH$_2$)^{47}Gly^{48}]hirudin$^{45-65}$ (designated as P79, DiMaio et al. (1991)) complexed with α-thrombin. The linker in the complex was largely exposed to the solvent outside of a deep groove between the active site and FRE and exhibited a large conformational flexibility without any strong interaction with thrombin (Yue et al., 1992; A. Zdanov, S. Wu, J. DiMaio, Y. Konishi, Y. Li, X. Wu, B. F. P. Edwards, P. D. Martin, & M. Cygler, manuscript in preparation).

We describe attempts to utilize the linker as a functional domain rather than as just a spacer. The linker was forced to lie down in the deep groove by shortening its length, and then peptide bonds were located at various positions in the linker with the expectation that they would form hydrogen bonds with thrombin S′ sites and improve the potency of the inhibitors.

[2] The numbering of the inhibitor residues is based on the hirudin sequence.

EXPERIMENTAL PROCEDURES

Materials. Human α-thrombin (3000 NIH units/mg), bovine fibrinogen (~75% of protein, 90% clottable), Tos-Gly-Pro-Arg-AMC·HCl salt, poly(ethylene glycol) 8000, and Ada were purchased from Sigma. AMC was obtained from Aldrich. Boc-Ada was prepared according to the procedure described by Chaturvedi et al. (1984). Boc-Bal, Boc-Abu, Boc-Aca, and Boc-Aha were purchased from BaChem. All other amino acid derivatives for peptide synthesis were purchased from Advanced ChemTech. The side chain protecting groups for Boc-amino acids were benzyl for Glu and Asp, tosyl for Arg, and 2-bromobenzyloxycarbonyl for Tyr. Boc-Gln-OCH$_2$-phenylacetylamidomethyl resin (0.73 mmol/g) was purchased from Applied Biosystems Inc. The solvents for peptide synthesis were obtained from B&J Chemicals and Applied Biosystems Inc. Tris and citric acid were purchased from Bio-Rad and Anachemia, respectively. HF and TFA were purchased from Matheson and Halocarbon Products Co., respectively.

Peptide Synthesis. The peptides were prepared according to the method described elsewhere (Szewczuk et al., 1992b), except P393, which used Orn side chain as a 6-atom linker. The C-terminal fragment of P393, H-Asp(Bzl)-Phe-Glu(Bzl)-Glu(Bzl)-Ile-Pro-Glu(Bzl)-Glu(Bzl)-Tyr(2-Br-Z)-Leu-Gln-PAM-resin, was synthesized by the Boc method (Szewczuk et al., 1992b), and then Fmoc-L-Orn(Boc)-OH was coupled to it using BOP reagent. The resin was washed three times with DMF, and the N-terminal amino group of Orn was deprotected with 50% piperidine in DMF, washed with DMF, and acetylated by acetic anhydride. The rest of the N-terminal fragment attached to the side chain of Orn was synthesized as described elsewhere using BOP as the coupling reagent (Szewczuk et al., 1992b). Final products were obtained as lyophilizates with 98% or higher purity estimated by analytical HPLC. The purified peptides were identified by amino acid analysis on a Beckman Model 6300 high-performance analyzer and by molecular weight analysis using an SCIEX API III mass spectrometer. Peptide contents in lyophilizates were determined by amino acid analysis.

Fibrin Clotting and Amidolytic Assays. The fibrin clotting assay was performed in 50 mM Tris-HCl buffer (pH 7.6 at 37 °C) containing 0.1 M NaCl and 0.1% poly(ethylene glycol) 8000 as reported elsewhere (Szewczuk et al., 1992b). The IC_{50} was estimated as the inhibitor concentration required to double the clotting time relative to the control.[3]

The inhibition of the amidolytic activity of human thrombin was measured spectrophotometrically using Tos-Gly-Pro-Arg-AMC as the fluorogenic substrate, as reported elsewhere (Szewczuk et al., 1992b). The concentrations of the substrate used in the amidolytic assay were 1–8 μM, and the concentrations of the inhibitors used were approximately in the range of 0.2–20-fold of K_i with 0.0067 NIH unit/mL of human thrombin. A nonlinear regression program, RNLIN in the IMSL library (IMSL, 1987), was used to estimate the kinetic parameters (K_s, V_{max}, K_i, and K_r).

Proteolytic Assays. The proteolytic stability of the inhibitors against human α-thrombin was measured using HPLC (Hewlett-Packard, Model 1090). An inhibitor (100 nmol) and the enzyme (100 pmol) were incubated at 37 °C in 4.0 mL of the buffer (50 mM Tris-HCl, pH 7.8). Aliquots of the reaction solution (1 mL) were removed at intervals, and the reaction was arrested by the addition of 10 μL of TFA and

[3] The inhibitor concentrations required to double the clotting time were 39% higher than those required to inhibit 50% of human α-thrombin at the enzyme concentration of 0.20 NIH unit/mL.

freeze-drying. The residues were dissolved in 150 μL of 1% TFA, injected directly onto a Vydac C_{18} (300-Å pore size, 0.46 × 25 cm) analytical column, and eluted with a linear gradient of acetonitrile containing 0.1% TFA from 10 to 70% over 60 min at a flow rate of 1 mL/min. The column eluent was monitored at 210 nm. The eluting peaks were collected and identified by amino acid analysis on the high-performance analyzer (Beckman Model 6300) and by mass spectrometry (SCIEX API III).

Molecular Dynamics Simulation. Molecular dynamics simulations were carried out on the linker segments of P151, P201, P239, P240, P312, and P336. The X-ray structure of human α-thrombin–P79 complex (Zdanov et al., manuscript in preparation) was used as a starting structure in the model. Using the program Quanta (version 32) (Polygen Corp.), the segment that spans Arg^{47} and Asp^{55} was replaced by Pro-Ada, Pro-Abu-Aha, Pro-Aha-Abu, Pro-Gly-Gly-Aca, Pro-Bal-Bal-Abu, and Pro-Bal-Gly-Gly-Gly to form P201, P151, P239, P240, P312, and P336, respectively. The active site and FRE inhibitor segments of the inhibitors were kept in the same positions as in the crystal structure of the thrombin–P79 complex to simulate the interactions of the linker with the thrombin S′ groove. The computations were performed using the CHARMm program (version 21.3) (Polygen Corp.), and the polar hydrogen force field (Brooks et al., 1983) was studied on a Iris 4D/280 (Silicon Graphics Inc).

The stochastic boundary molecular dynamics procedure (Brünger et al., 1987; Brooks & Karplus, 1989) was used in an approximately spherical reaction region of the linker–thrombin structure with a radius of 13 Å surrounded by a 2-Å buffer region. The reaction sphere included the inhibitor segments, 46–57, as well as thrombin residues: 16–17, 30–44, 57–58, 60D–60F, 60H, 64, 67, 70, 72–74, 139–156, 190–197, 213, and 220.[4] The space inside the sphere was filled with water by overlaying a previously equilibrated box of TIP3P (Jorgensen et al., 1983) water molecules. Water molecules within 2.6 Å of either thrombin or peptide were removed from the system. A constant dielectric function ($\epsilon = 1$) and a cutoff distance of 10.0 Å for both the van der Waals and the electrostatic terms were used. The temperature was maintained at 300 ± 5 K by coupling all non-hydrogen atoms in the buffer region to a Langevin heat bath. The SHAKE program (Ryckaert et al., 1977) was employed to keep the bonds involving hydrogen atoms fixed at their equilibrium positions. The time step was 1.5 fs. After a 8000-step equilibration of the water structure in the presence of the fixed protein and peptide molecules and a 20 000-step equilibration of water, protein, and peptide structures, a second TIP3P water overlay was applied to fill any void in the solvent. A 100 000-step (150 ps) dynamics simulation was carried out with data collection at every 40 steps. The trajectory data collected from dynamics simulations were visualized using Quanta under the dynamics manipulation option. Another simulation was carried out for each inhibitor using a different random number to generate another Boltzmann distribution of initial velocity with a duration to 300 ps. Atomic fluctuation of the linkers was estimated as the rms deviation of each linker atom from the average structure.

RESULTS AND DISCUSSION

The six-residue linker, $hirudin^{49-54}$, of N^{α}-acetyl[D-Phe^{45},Arg^{47}]$hirudin^{45-65}$ (P53) was substituted by various linkers. We focused herein on the linker backbone only; thus, the linkers synthesized contained no side chain and were expressed as the number of atoms contributing to the length of the linkers, e.g., a linker of 4-aminobutyric acid is a 5-atom linker. The linkers were composed of various combinations of Gly (3 atoms), Bal (4 atoms), Abu (5 atoms), L-Orn (6 atoms), Aca (7 atoms), Aha (8 atoms), and Ada (13 atoms), where the length of the linker is expressed with the number of atoms in parentheses. This allowed precise manipulation of their ultimate lengths from 6- to 18-atom linkers. Furthermore, various numbers and locations of the amide bonds in the linker were designed to explore possible interactions with thrombin. The structures of the synthesized linkers are shown in Table I.

Inhibition Mechanism. We propose the inhibition mechanism of bivalent inhibitors (Scheme I) to reflect the observations in this article. In Scheme I, thrombin (E) binds to a substrate (S) with a dissociation constant, K_s, and hydrolyzes it to products (P) with a kinetic constant, k_p. The inhibitor (I) rapidly binds to the thrombin FRE with a dissociation constant, K_i', and forms a complex, EI (Jackman et al., 1992). The inhibitor bound to thrombin FRE enhances the binding of the substrate, Tos-Gly-Pro-Arg-AMC, 1.6-fold without affecting the kinetic constant, k_p (Naski et al., 1990; Dennis et al., 1990; Hortin & Trimpe, 1991). Since the inhibitor contains an active site inhibitor segment, EI is in equlibrium with another form of complex, EI*, in which the inhibitor binds not only to FRE but also to the active site. K_r is the equilibrium constant between EI and EI*. The active site inhibitor segment in EI* binds to the active site in a substrate binding mode and is slowly hydrolyzed to P* with a kinetic constant, k_i, where $k_i \ll k_p$.

Scheme I matches well with the following observations: (1) Most of the inhibitors with the 13–18-atom linkers, which have linkers more than long enough to span the active site and the FRE inhibitor segments, showed a competitive inhibition toward the small substrate. This is the case where the equilibrium between EI and EI* is completely shifted to EI*, i.e., $K_r \approx 0$. Thrombin in the EI* form hydrolyzes the inhibitor very slowly (negligible within a few minutes of reaction time for the fluorogenic assay) but not the fluorogenic substrate. Consequently, the inhibitors competitively block the hydrolysis of the fluorogenic substrate. (2) Some of the bivalent inhibitors with 11–13-atom linkers (P115, P148, P239, and P282) showed a hyperbolic inhibition (Baici, 1987), i.e., saturating reciprocal velocities with increasing inhibitor concentration, up to a limiting value beyond which no further inhibition was observed (Figure 1). This means that a portion of the thrombin molecules form a ternary complex (ESI) comprising thrombin, the small active site directed substrate, and the inhibitor. The residues D-Phe-Pro-Arg of the inhibitor do not occupy the thrombin active site in EI and ESI complexes. It may be exposed to the solvent and have almost no interaction with thrombin, because no other binding sites of D-Phe-Pro-Arg on thrombin have so far been identified. Then, the bivalent inhibitor in EI and ESI complexes should bind to thrombin predominantly through FRE, and K_i' values in Scheme I should be close to the IC_{50} (1.7 ± 0.2 μM) value of the FRE inhibitor, N^{α}-acetylhirudin$^{55-65}$ (Szewczuk et al., 1992b). This was confirmed when the kinetic data of hyperbolic inhibitors were analyzed as described below. (3) When the linker is too short to span the active site and the FRE inhibitor segments, only EI (but not EI*) is formed. This is due to a higher affinity of the FRE inhibitor segment than the active site inhibitor segment to α-thrombin (Maraganore et al., 1990; Yue et al.,

[4] The numbering of human α-thrombin residues is based on the chymotrypsin sequence.

Table I: Activities of Thrombin Inhibitors

A. Activities of Thrombin Inhibitors with 14 - 18 Atom Linkers

Peptide	Structure of linker[a]	Activities IC_{50}[b] [nM]	K_i[c] [nM]	$1/K_r$[d]
P53[e]	Gln-Ser-His-Asn-Asp-Gly	28 ± 2	5.5 ± 0.4	45 ± 19
P199	Gly Gly Gly Gly Gly Gly	12 ± 1	1.7 ± 0.3	>65
P146	Aha Aha	20 ± 3	3.4 ± 0.2	>65
P198	Gly Gly Gly Gly Gly	16 ± 2	2.4 ± 0.3	>65
P145	Aha Aca	12 ± 1	2.8 ± 0.4	>65
P147	Aca Aca	16 ± 1	2.3 ± 0.3	>65
P338	Aca Gly Bal	4.5 ± 0.6	1.7 ± 0.3	>65
P337	Bal Gly Aca	8.9 ± 1.3	2.6 ± 0.4	>65

Number of atom of the linker

B. Activities of Thrombin Inhibitors with 13 Atom Linkers

Peptide	Structure of linker[a]	Activities IC_{50}[b] [nM]	K_i[c] [nM]	$1/K_r$[d]
P201	Ada	17 ± 3	2.6 ± 0.3	>65
P151	Aha Abu	6.0 ± 0.8	0.82 ± 0.02	>65
P239	Abu Aha	150 ± 20	25 ± 3	36 ± 5
P335	Aca Gly Gly	4.5 ± 0.5	1.2 ± 0.1	>65
P240	Gly Aca Gly	94 ± 9	11 ± 1	>65
P333	Gly Gly Aca	40 ± 4	14 ± 1	>65
P334	Abu Gly Abu	29 ± 1	7.6 ± 0.3	>65
P312	Bal Bal Abu	16 ± 1	4.9 ± 1.1	>65
P336	Bal Gly Gly Gly	2.5 ± 0.2	0.64 ± 0.13	>65
P393	Bal Gly Orn NH-Ac	2.9 ± 0.2	0.51 ± 0.05	>65

C. Activities of Thrombin Inhibitors with 11 - 12 Atom Linkers

Peptide	Structure of linker[a]	Activities IC_{50}[b] [nM]	K_i[c] [nM]	$1/K_r$[d]
P331	Bal Gly Abu	10 ± 1	2.7 ± 0.3	>65
P332	Abu Gly Bal	22 ± 2	4.8 ± 0.5	>65
P115[e]	Gly Gly Gly Gly	140 ± 20	40 ± 1	21 ± 5
P148	Aca Abu	380 ± 30	105 ± 13	9.9 ± 0.5
P282	Aha Gly	97 ± 10	28 ± 2	14 ± 1.0

Number of atom of the linker

D. Activities of Thrombin Inhibitors with 6 - 10 Atom Linkers

Peptide	Structure of linker[a]	Activities IC_{50}[b] [nM]	K_i[c] [nM]
P149	Abu Abu	3200 ± 100	ni[f]
P114[e]	Gly Gly Gly	2000 ± 100	ni
P150	Aha	6700 ± 700	ni
P83[e]	Gly Gly	2790 ± 95	ni

Number of atom of the linker

[a] The active site and the FRE inhibitors (Ac(dF)PRP and DFEEIPEEYLQ-OH, respectively) remain the same in all peptides in this study. [b] Inhibitions of human thrombin-mediated fibrin clot formation. The clotting assay was performed as described in the Experimental Procedures. IC_{50} is defined as the inhibitor concentration required to double the clotting time relative to the control. Means are of three determinants ± SEM. [c] Inhibition of amidolytic activity of human thrombin. The fluorogenic assay using Tos-Gly-Pro-Arg-AMC as a substrate was performed as described in the Experimental Procedures. Means are of three determinants ± SEM. [d] K_r is defined in Scheme I and was estimated from eq 1. [e] The activities of the inhibitors, P83, P114, and P115, were reported previously (Yue et al., 1992). [f] No inhibition was observed even at 0.1 mM inhibitor concentration.

1992). Such inhibitors with short linkers should have no inhibition toward the small substrate, but should be active in the clotting assay in which the substrate, fibrinogen, binds to the FRE as well as to the active site of thrombin. The inhibitors with short 6–10-atom linkers showed the expected activities, i.e., no inhibition in the fluorogenic assay and a weak inhibition in the clotting assay with an IC_{50} in the micromolar range, which is close to that of the FRE inhibitor, N^{α}-acetyl-hirudin$^{55-65}$. Consequently, Scheme I reflects well the three types of inhibitions observed in this study.

Scheme I was kinetically analyzed as follows: In the fluorogenic assay, the inhibitor was used in a large excess to thrombin and the degradation of the inhibitor by thrombin was negligible during the assay. The variation of initial velocity

Scheme I

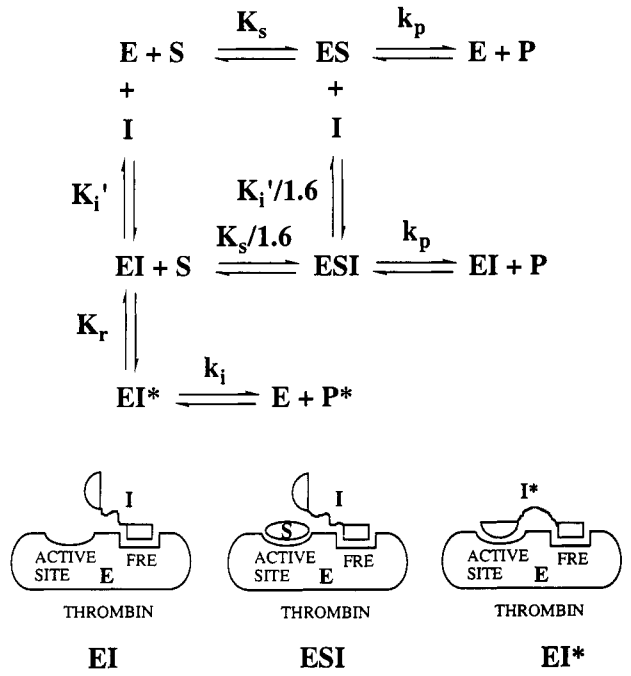

(v) of fluorescence change at an inhibitor concentration [I] is expressed as

$$v = V_{max}\{[S]/K_s + 1.6[I][S]/K_sK_i'\}/\{1 + [S]/K_s + (1 + 1/K_r)[I]/K_i' + 1.6[I][S]/K_sK_i'\} \quad (1)$$

where V_{max} is the maximum velocity of the enzyme. The inhibition constant of the active site is expressed as

$$K_i = [E][I]/[EI^*] = K_i'K_r \quad (2)$$

The initial velocity of the fluorescence change was recorded at various concentrations of the substrate and the inhibitor. The data were analyzed using a nonlinear regression program, RNLIN in the IMSL library (IMSL, 1987), to estimate the kinetic parameters (K_s, V_{max}, K_i, and K_r), and the results are listed in Table I. The K_s and V_{max} values observed in the assays of the inhibitors in Table I were 3.1 ± 0.9 μM and 1.3 ± 0.5 μM/min, respectively. K_i' values were estimated for hyperbolic inhibitors. These were 0.84, 1.04, 0.90, and 0.39 μM for P115, P148, P239, and P282, respectively, and are close to the IC_{50} (= 1.7 ± 0.2 μM) value of the FRE inhibitor, N^{α}-acetylhirudin$^{55-65}$ (Szewczuk et al., 1992b).

The cleavage of the inhibitors by thrombin was analyzed using HPLC as described in the Experimental Procedures. Since the initial concentration of the inhibitor (= 25 μM) ≫ K_i and K_r ≪ 1, almost all of the thrombin molecules are in the EI* complex during the assay. The product formed at time t is

$$[P^*] = k_i[EI^*]t \approx k_i[E]_T t \quad (3)$$

where $[E]_T$ (= 25 nM) is the total concentration of the enzyme. The k_i values of the inhibitors were estimated from the amounts of the peptides cleaved by thrombin at certain reaction times and are listed in Table II. It is interesting that P53 with the linker of the hirudin sequence is more readily cleaved by thrombin than the inhibitors with the linkers of ω-amino acids. The linkers of P239, P148, and P282, which induced a hyperbolic inhibition, further increased the proteolytic stability of the inhibitors against thrombin. The active site inhibitor segment in these inhibitors might be slightly distorted from the substrate binding mode as discussed below for P239.

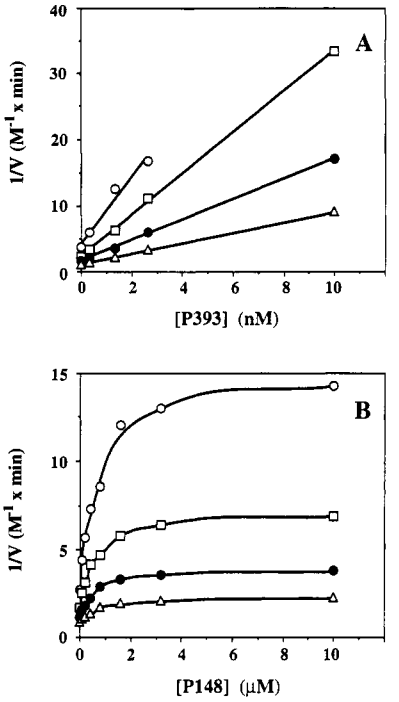

FIGURE 1: Dixon plots of the competitive and hyperbolic inhibitions of human α-thrombin (0.0067 NIH unit/mL) by (A) P393 (K_i = 0.51 ± 0.05 nM and $1/K_r > 65$) and (B) P148 (K_i = 0.112 ± 0.014 μM and $1/K_r$ = 5.8 ● 0.3), respectively. The fluorogenic assay was performed using Tos-Gly-Pro-Arg-AMC (K_s = 3.5 μM and V_{max} = 1.4 μM/min) as a substrate at the concentrations of 1 (○), 2 (□), 4 (●), and 8 μM (△) at pH 7.8 and 25 °C.

Table II: Proteolytic Stability of the Inhibitors against α-Thrombin

peptide	linker	length of the linker[a]	incubation time (h) 5	10	24	$k_i \times 10^3$ (s^{-1})
P53	QSHNDG	18	30[b]	55	100	16 ± 1
P146	Aha-Aha	16	14	27	53	7.1 ± 0.7
P147	Aca-Aca	14	12	21	51	6.1 ± 0.4
P151	Aha-Abu	13	14	23	57	6.9 ± 0.6
P239	Abu-Aha	13	7	14	31	3.8 ± 0.1
P312	Bal-Bal-Abu	13	14	26	56	7.2 ± 0.5
P148	Aca-Abu	12	3	5	11	1.5 ± 0.2
P282	Aha-Gly	11	5	10	21	2.7 ± 0.2
P149	Abu-Abu	10	<1	<1	<1	
P150	Aha	8	<1	<1	<1	

[a] The length of the linker is expressed as the number of the atoms in the main chain. [b] The percentage of the inhibitors hydrolyzed by thrombin was estimated from the peak areas in HPLC profiles.

Interestingly, thrombin failed to cleave the inhibitors with an 8- or 10-atom linker even though they have the same active site inhibitor segment, D-Phe-Pro-Arg-Pro, suggesting that the 8- or 10-atom linker is too short to bridge the active site and FRE inhibitor segments. Consistently, these inhibitors failed to block the thrombin active site as described below. It should be mentioned that the inhibitors with linkers shorter than 13 atoms gained their slower turnover or no cleavage by thrombin at the expense of a significant potency loss, as described below.

Length of Linker. The analogs with 14–18-atom linkers (P145, P146, P147, P198, P199, P337, and P338) showed a competitive inhibition with potencies in the nanomolar range (K_i = 1.7–3.4 nM, IC_{50} = 9–20 nM) (Table IA). The inhibitors with longer linkers ([Gly]$_6$-Asp-Gly (24 atoms) and [Gly]$_8$-Asp-Gly (30 atoms)) also showed similar potencies (K_i = 3.0 and 2.6 nM, respectively) (Maraganore et al., 1990). Thus, the length of 14 atoms is long enough to link the active site and the FRE inhibitor segments. The excess atoms in the

longer linker seem to be largely exposed to the solvent outside of a groove between the active site and the FRE without contributing to the binding as observed in the thrombin–hirudin (Rydel et al., 1990) and thrombin–P79 complexes (Zdanov et al., manuscript in preparation).

The use of a shorter 13-atom linker may force the linker segment to lie deeper in the S′ groove and to be positioned closer to the thrombin residues in this groove. Indeed, we observed a strong dependence of potency on the chemical structure of the linker (Table IB). In particular, the potency was affected by the location and the number of peptide bonds in the linker. We took an inhibitor, P201, which has no peptide bond in the linker, as our reference state for evaluating the effects of the peptide bonds in the linker. The potencies of P201 (K_i = 2.6 ± 0.3 nM and IC_{50} = 17 ± 3 nM) are comparable to those of inhibitors with 14–18-atom linkers. In the following, we organize our results with respect to the peptide bond position in the linker. The peptide bond position is referred to as linker^{m-n}, where m and n are the positions of the amide C′ and N atoms, respectively, in the linker.

(1) Peptide bond at linker$^{8-9}$: An inhibitor, P151, which incorporated a peptide bond at linker$^{8-9}$, showed a potency of K_i = 0.82 ± 0.02 nM and an IC_{50} = 6.0 ± 0.8 nM. This improved the K_i and IC_{50} values 3.2- and 2.8-fold, respectively, from those of the reference inhibitor, P201. This suggested the occurrence of favorable interactions between the peptide bond at linker$^{8-9}$ and thrombin.

(2) Peptide bond at linker$^{5-6}$: In contrast to P151, the incorporation of a peptide bond at linker$^{5-6}$ (P239) increased the K_i and IC_{50} values 9.6- and 8.8-fold, respectively, suggesting some unfavorable interactions between the peptide bond at linker$^{5-6}$ and thrombin. We also examined an inhibitor, P334, with peptide bonds at both linker$^{5-6}$ and linker$^{8-9}$. If we assume an additive effect of the peptide bonds in P151 and P239, the K_i and IC_{50} values of P334 were expected to be 7.9 and 53 nM, respectively. These are close to the observed K_i and IC_{50} values of 7.6 ± 0.3 and 29 ± 1 nM, respectively.

(3) Peptide bond at linker$^{4-5}$: Two peptides that differ only at the linker$^{4-5}$ peptide bond were compared. Both P335 and P336 contain peptide bonds at linker$^{7-8}$ and linker$^{10-11}$ (Table IB). In addition, P336 contains a third peptide bond at linker$^{4-5}$. This extra peptide bond resulted in improved potency of P336 (K_i = 0.64 ± 0.13 nM, IC_{50} = 2.5 ± 0.2 nM) over P335 (K_i = 1.2 ± 0.1 nM, IC_{50} = 4.5 ± 0.5 nM). On the other hand, an examination of two peptides, P151 and P312, that also differ only at the linker$^{4-5}$ peptide bond yielded opposite results. Both P151 and P312 contain a peptide bond at linker$^{8-9}$ (Table IB). In addition, P312 contains a second peptide bond at liner$^{4-5}$. This extra peptide bond resulted in lower potency of P312 (K_i = 4.9 ± 1.1 nM, IC_{50} = 16 ± 1 nM) over P151 (K_i = 0.82 ± 0.02 nM, IC_{50} = 6.0 ± 0.8 nM). These two apparently contradictory results suggest that it is possible to find an orientation of the peptide bond with good interaction with thrombin but that the requirements for favorable orientations of both the linker$^{4-5}$ and linker$^{8-9}$ peptide bonds are mutually incompatible. These favorable and unfavorable effects of the peptide bond at linker$^{4-5}$ were investigated further using molecular dynamics simulations in the section on Molecular Dynamics, where possible hydrogen-bonding models are presented.

(4) Peptide bond at liner$^{10-11}$: P393, which has the same linker as P336 minus the linker$^{10-11}$ peptide bond, showed the same potency as P336. This indicates no net contribution of a peptide bond in this position to the inhibitor potency.

(5) Peptide bond at linker$^{6-7}$: P240 and P333 have a peptide bond at linker$^{3-4}$ in common, but differ by linker$^{10-11}$ and linker$^{6-7}$, respectively. They showed essentially the same K_i. Since the peptide bond at linker$^{10-11}$ was indicated to have little effect on the inhibitor potency, the comparable potency of P240 and P333 suggested the small effect of the peptide bond at linker$^{6-7}$ in the binding to thrombin.

(6) Peptide bond at linker$^{3-4}$: If the net contributions of the peptide bonds at linker$^{6-7}$ and linker$^{10-11}$ are small as suggested above, the weak potency of P240 and P333 may be due to the unfavorable interaction of the peptide bond at linker$^{3-4}$ with thrombin. This was investigated further using molecular dynamics simulations in the section on Molecular Dynamics.

These results implied that, while the interactions of the peptide bonds of the 13-atom linkers with thrombin at linker$^{3-4}$ and linker$^{5-6}$ were unfavorable, those at linker$^{7-8}$ and linker$^{8-9}$ were favorable, whereas the peptide bonds at linker$^{6-7}$ and linker$^{10-11}$ had little effect. It should be emphasized that these implications are only for 13-atom linkers. Most of the inhibitors with a 13-atom linker showed a competitive inhibition, suggesting that these 13-atom linkers are long enough to bridge the active site and the FRE inhibitor segments with no distortion of the active site inhibitor segment. P239 was not only the poorest inhibitor of those with 13-atom linkers but was also the only one which showed a hyperbolic inhibition with a slower cleavage rate by thrombin. Further structural studies by molecular dynamics simulation are described below.

The potency of the inhibitors with 12-atom linkers also showed a strong dependence on the chemical structure of the linker (Table IC). Unlike the 13-atom linkers, the peptide bond at linker$^{7-8}$ in P148 strongly affected the potency, resulting in K_i = 112 ± 14 nM and IC_{50} = 380 nM. However, further incorporation of a peptide bond at linker$^{4-5}$ (P331) improved the potency drastically to K_i = 2.7 ± 0.3 nM and IC_{50} = 10 ± 1 nM, suggesting strong favorable interactions of the peptide bond at linker$^{4-5}$ with thrombin. P331 and P332 showed competitive inhibition, suggesting that the 12-atom linkers are long enough to bridge the active site and the FRE inhibitor segments without distorting the active site inhibitor segment. However, unfavorable interactions of the linker of P148 with thrombin might distort the binding mode of the active site inhibitor segment, resulting in poor and hyperbolic inhibition (Figure 1) and a slow cleavage rate by thrombin.

The inhibitor, P282, with an 11-atom linker could bridge the active site and the FRE inhibitor segments with a resonably strong potency of K_i = 29 ± 3 nM and an IC_{50} = 97 ± 10 nM (Table IC). Its hyperbolic inhibition and slow cleavage by thrombin suggested some distortion in the binding mode of the active site inhibitor segment to thrombin. The inhibitors with 6–10-atom linkers (P149, P114, P150, and P83) showed no inhibition at the thrombin active site (Table ID). Furthermore, their potency is close to that (IC_{50} = 1.7 ± 0.2 μM) of the FRE inhibitor, N^{α}-acetylhirudin$^{55-65}$ (Szewczuk et al., 1992b), suggesting that they predominantly interact at the FRE of thrombin. The thermodynamic study of these inhibitors is described elsewhere (Hopfner et al., 1993). In summary, the linker may require a minimum of 11 atoms to bridge the active site and FRE inhibitor segments, 12 atoms to bridge them without distortion, and 13 atoms to optimize the interaction with thrombin.

Molecular Dynamics Simulations. In order to investigate the structural basis of the variation of potency with respect to the chemical structure of the linker, molecular dynamics simulations were carried out on some of these inhibitors with

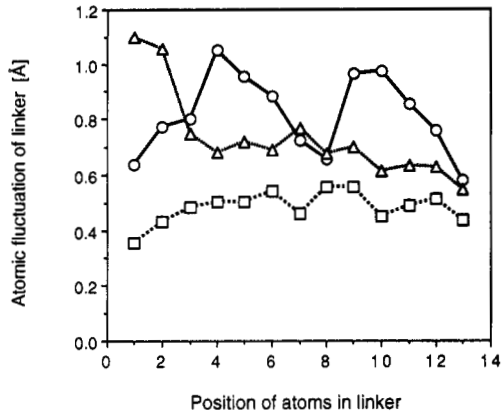

FIGURE 2: Atomic fluctuations of the linkers in P201 (○), P240 (△), and P336 (□), estimated as the rms deviation of each linker atom from their average structures.

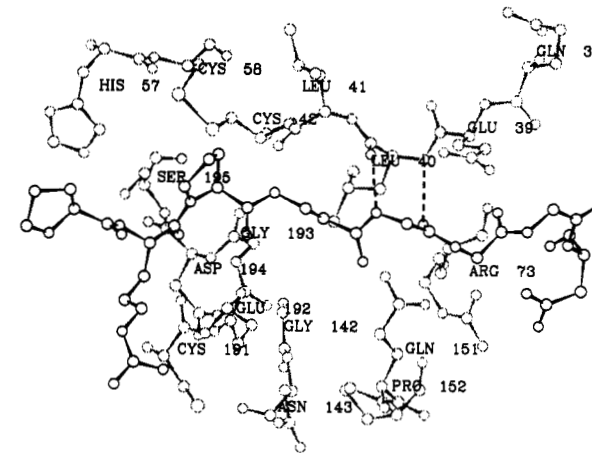

FIGURE 3: Average structures of the linker portions of P336 in the complex with human α-thrombin obtained from molecular dynamics simulations. The linker of P336 formed two stable hydrogen bonds between NH at linker^5 and the carbonyl oxygen of thrombin Leu^{40} and between the carbonyl oxygen at linker^7 and NH of thrombin Leu^{40}, resulting anti-parallel β-sheet-like hydrogen bonds between Gly at linker$^{5-7}$ and thrombin Leu^{40} (thick lines). The structure of α-thrombin in this region is shown with thin lines. The hydrogen bonds are shown with dashed lines.

13-atom linkers. Particular attention was paid to the formation or absence of hydrogen bonds involving peptide bonds at positions 3–4, 4–5, 5–6, 7–8, 8–9, and 10–11 of the linker. The inhibitors that were used in the simulations were P151, P201, P239, P240, P312, and P336. In the following, we organize our results with respect to the peptide bond position in the linker.

(1) No amide bond: P201, with no linker amide bond, showed large fluctuations at linker$^{4-6}$ and linker$^{9-11}$ and moderate fluctuations at linker$^{7-8}$ during the molecular dynamics simulation (Figure 2), although no specific interaction of methylene groups at linker^7 and linker^8 with thrombin was indicated in the simulation. This large fluctuation of the linker and no indication of specific interaction with thrombin support our choice of P201 as a reference state for evaluating the effects of the peptide bonds in the linker.

(2) Peptide bond at linker$^{3-4}$: The peptide bond at linker$^{3-4}$ in P240 failed to form any hydrogen bond with thrombin and induced a large conformational fluctuation at linker$^{1-2}$ (Figure 2). The polar amide group may not be favored in the P_2' position. The peptide bond at linker$^{10-11}$ in P240 also failed to form any hydrogen bond with thrombin.

(3) Peptide bond at linker$^{4-5}$: As described above, a peptide bond at linker$^{4-5}$ showed a mixed effect, i.e., it improved the potency in P336, but it adversely affected the potency in P312. Molecular dynamics simulation of P336 indicated a strong hydrogen bond between the NH at linker^5 and the carbonyl oxygen of the Leu^{40} of thrombin, which could explain the improved potency of this inhibitor (Figure 3). The carbonyl group at linker^4 showed no indication of interaction with thrombin. As described below, the carbonyl oxygen at linker^7 of P336 forms a hydrogen bond with the NH of Leu^{40} of thrombin. Interestingly, the carbonyl oxygen at linker^8 of P312 also forms a hydrogen bond with the NH of Leu^{40} of thrombin. This hydrogen bond shifted the position of the peptide bond at linker$^{4-5}$ of P312 to the corresponding position of liner$^{3-4}$ of P336 in the complex with thrombin. Because of the shifted position, the peptide bond at linker$^{4-5}$ of P312 showed no specific interaction with thrombin in the molecular dynamics simulation.

(4) Peptide bond at linker$^{5-6}$: Since the NH at linker^5 can make a strong hydrogen bond with the carbonyl oxygen of Leu^{40} of thrombin, the replacement of the NH at linker^5 with the carbonyl group in P239 may cause an unfavorable interaction between the carbonyl groups at linker^5 and in thrombin Leu^{40}. Indeed, the carbonyl group at linker^5 shifted toward the FRE after 70 ps of molecular dynamics simulation to avoid the repulsive dipole–dipole interaction and formed a strong hydrogen bond with the NH of Leu^{40}. In consequence, the N-terminal side of the linker was stretched out and the carbonyl carbon of Arg^{47} of the inhibitor was shifted approximately 0.8 Å toward the FRE. The characteristics of P239 such as low potency, hyperbolic inhibition, and slow cleavage by thrombin may be due to this distorted conformation of the active site inhibitor segment.

(5) Peptide bond at linker$^{7-8}$: Molecular dynamics simulation indicated that the carbonyl oxygen at linker^7 in P336 forms a strong hydrogen bond with the NH of Leu^{40} of thrombin. The same type of hydrogen bond was observed between a carbonyl oxygen of a linker of a hirudin-based bivalent inhibitor, hirutonin IIIb, and the NH of thrombin Leu^{40} in the crystal structure of the thrombin–hirutonin IIIb complex (Zdanov et al., manuscript in preparation). This and another hydrogen bond between NH at linker^5 and the carbonyl oxygen of Leu^{40} of thrombin form antiparallel β-sheet-like hydrogen bonds between Gly in the linker and Leu^{40} of thrombin (Figure 3). The stable β-sheet-like hydrogen bonds restrict the conformational flexibility of the entire region of the linker (Figure 2). Apparently, the enthalpic gain from the β-sheet-like hydrogen bond formation overcomes the entropy loss of the linker upon complex formation, leading to the high observed potency of P336.

(6) Peptide bond at linker$^{8-9}$: P151 has a peptide bond at linker$^{8-9}$. In the molecular dynamics simulation, the linker of P151 was oscillating between two distinctive conformers approximately every 70 ps. One conformer contained a hydrogen bond between the carbonyl oxygen at linker^8 and NH of thrombin Leu^{40}, while the NH at linker^9 was pointing toward the solvent (Figure 4A). The other conformer contained a hydrogen bond between the carbonyl group at linker^8 and the N$^{\epsilon}$H of the Gln^{151} side chain of thrombin (Figure 4B). The high potency of P151 appears to be due to these hydrogen bonds. P312, which has a peptide bond at linker$^{8-9}$, also formed the same hydrogen bond as the former one between the carbonyl oxygen at linker^8 and NH of thrombin Leu^{40}. The effect of this hydrogen bond to the peptide bond at linker$^{4-5}$ is described above. The latter hydrogen bond of P151 with the N$^{\epsilon}$H of the Gln^{151} side chain of thrombin was not observed in the case of P312.

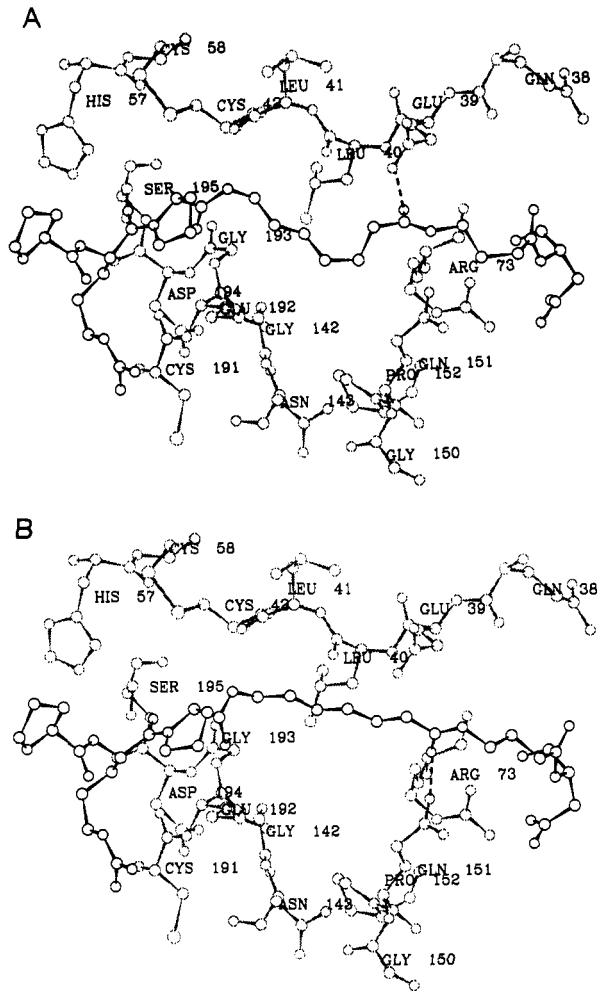

FIGURE 4: Average structures of the linker portions of P151 in the complex with human α-thrombin obtained from molecular dynamics simulations. The linker of P151 oscillated between two stable conformers every 70 ps. Average structures of the two stable conformers of P151 are shown in A and B. The structure of α-thrombin in this region is shown with thin lines. One conformer forms a hydrogen bond between the carbonyl oxygen at linker^8 and NH of thrombin Leu^{40} (A). The other conformer forms a hydrogen bond between the carbonyl oxygen at linker^8 and the side chain N$^{\epsilon}$H of thrombin Gln^{151} (B). The hydrogen bonds are shown with dashed lines.

(7) Peptide bond at linker$^{10-11}$: Molecular dynamics simulation of P336 showed no specific interactions between the peptide bond at linker$^{10-11}$ and thrombin. This supports the above analysis that this peptide bond has little effect on the binding to thrombin.

The role of thrombin's Leu^{40}: The overall picture that emerges from the molecular dynamics simulations is that the Leu^{40} backbone carbonyl and NH groups play a key role in mediating the specific interactions of thrombin with the linker segment. Favorable locations in the linker for hydrogen bonding to Leu^{40} are linker^7 for the carbonyl group and linker^5 for the NH group, as in P336 and P393, or linker^8 for the carbonyl group as in P151. In any of the molecular dynamics simulations of thrombin–inhibitor (P151, P201, P239, P240, P312, or P336) complexes, no water molecules were observed in the groove at the S′ site, and Leu^{40} formed no hydrogen bonds with water molecules. Consequently, the inhibitors, P151, P336, and P393, formed good hydrogen bonds with Leu^{40} with a net gain of interaction energy and exhibited improved potencies.

CONCLUSIONS

The minimum lengths of the linker required to span the active site and the FRE inhibitor segments were 11 atoms with some distortion and 12 atoms without distortion. The inhibitors with a 13-atom linker showed the highest potency of up to 0.51 ± 0.05 nM, which is 11-fold more potent than the inhibitor (P53) with the linker of hirudin sequence (QSHNDG). Molecular dynamics simulations indicated that the improvements in the potencies of the inhibitors were mainly due to the hydrogen bond formation of thrombin's Leu^{40} with linker^7 carbonyl and linker^5 NH groups, as in P336 and P393, or with linker^8 carbonyl group as in P151. Consequently, these inhibitors (P151, P336, and P393) are no longer bivalent inhibitors; instead, they may be classified in a family of multivalent inhibitors.

ACKNOWLEDGMENT

We thank Dr. Andrew Storer for the helpful discussions. Thanks are also due to Virginia Laoun, Jean Lefebvre, Lynne LeSauteur, and Sean Taylor for their excellent technical assistance.

REFERENCES

Agnelli, G., Pascucci, C., Cosmi, B., & Nenci, G. G. (1991) *Thromb. Haemostasis 66*, 592–597.

Badimon, L., Merino, A., Badimon, J., Chesebro, J. H., & Fuster, V. (1991) *Trends Cardiovasc. Med. 1*, 261–267.

Baici, A. (1987) *Biochem. J. 244*, 793–796.

Bajusz, S., Barabas, E., Tolnay, P., Széll, E., & Bagdy, D. (1978) *Int. J. Pept. Protein Res. 12*, 217–221.

Bourdon, P., Jablonski, J.-A., Chao, B. H., & Maraganore, J. M. (1991) *FEBS Lett. 294*, 163–166.

Brooks, C. L., III, & Karplus, M. (1989) *J. Mol. Biol. 208*, 159–181.

Brooks, C. L., III, Bruccoleri, R. E., Olafson, B. D., States, D. J., Swaminathan, S., & Karplus, M. (1983) *J. Comput. Chem. 4*, 187–217.

Brünger, A. T., Huber, R., & Karplus, M. (1987) *Biochemistry 26*, 5153–5162.

Chaturvedi, D. N., Knittel, J. J., Hruby, V. J., Castrucci, A. M., & Hadley, M. E. (1984) *J. Med. Chem. 27*, 1406–1410.

Chesebro, J. H., Knatterud, G., Roberts, R., Borer, J., Cohen, L. S., Dalen, J., Dodge, H. T., Francis, C. K., Hillis, D., Ludbrook, P., Markis, J. E., Mueller, H., Passamani, E. R., Powers, E. R., Rao, A. K., Robertson, T., Ross, A., Ryan, T. J., Sobel, B. E., Willerson, J., Williams, D. O., Zaret, B. L., & Braunwald, E. (1987) *Circulation 76*, 142–154.

Dennis, S., Wallace, A., Hofsteenge, J., & Stone, S. R. (1990) *Eur. J. Biochem. 188*, 61–66.

DiMaio, J., Gibbs, B., Munn, D., Lefebvre, J., Ni, F., & Konishi, Y. (1990) *J. Biol. Chem. 265*, 21698–21703.

DiMaio, J., Ni, F., Gibbs, B., & Konishi, Y. (1991) *FEBS Lett. 282*, 47–52.

DiMaio, J., Gibbs, B., Lefebvre, J., Konishi, Y., Munn, D., Yue, S.-Y., & Hornberger, W. (1992) *J. Med. Chem. 35*, 3331–3341.

Fenton, J. W., II, Ofosu, F. A., Moon, D. G., & Maraganore, J. M. (1991a) *Blood Coagulation Fibrinolysis 2*, 69–75.

Fenton, J. W., II, Villanueva, G. B., Ofosu, F. A., & Maraganore, J. M. (1991b) *Haemostasis 21* (Suppl. No. 1), 27–31.

Hogg, P. J., & Jackson, C. M. (1989) *Proc. Natl. Acad. Sci. U.S.A. 86*, 3619–3623.

Hopfner, K.-P., Ayala, Y., Szewczuk, Z., Konishi, Y., & Di Cera, E. (1993) *Biochemistry* (in press).

Hortin, G. L., & Trimpe, B. L. (1991) *J. Biol. Chem. 266*, 6866–6871.

IMSL, International Mathematical Statistical Library (1987) *Library Reference Manual*, 9th ed., version 1.0, 2500 City West, Houston, TX 77042.

Jackman, M. P., Parry, M. A. A., Hofsteenge, J., & Stone, S. R. (1992) *J. Biol. Chem. 267*, 15375–15383.

Jakubowski, J. A., & Maraganore, J. M. (1990) *Blood 75*, 399–406.

Jorgensen, W. L., Chandrasekhar, J., Madura, J., Impey, R. W., & Klein, M. L. (1983) *J. Chem. Phys. 79*, 926–935.

Kettner, C., & Shaw, E. (1979) *Thromb. Res. 14*, 969–973.

Knadler, M. P., Ackermann, B. L., Coutant, J. E., & Hurst, G. H. (1992) *Drug Metab. Dipos. 20*, 89–95.

Krstenansky, J. L., Broersma, R. J., Owen, T. J., Payne, M. H., Yates, M. T., & Mao, S. J. (1990) *Thromb. Haemostasis 63*, 208–214.

Mao, S. J. T., Yates, M. T., Owen, T. J., & Krstenansky, J. L. (1988) *Biochemistry 27*, 8170–8173.

Maraganore, J. M., Chao, B., Joseph, M. L., Jablonsky, J., & Ramachandran, K. L. (1989) *J. Biol. Chem. 264*, 8692–8698.

Maraganore, J. M., Bourdon, P., Jablonsky, J., Ramachandran, K. L., & Fenton, J. W., II (1990) *Biochemistry 29*, 7095–7101.

Marder, V. J., & Sherry, S. (1988) *New Engl. J. Med. 318*, 1512–1520.

Markwardt, F., Nowak, G., Sturzebecher, J., Griessbach, U., Walsmann P., & Volgel, G. (1984) *Thromb. Haemostasis 52*, 160–163.

Munkvad, S., Gram, J., & Jespersen, J. (1991) *Scand. J. Clin. Lab. Invest. 51*, 581–590.

Naski, M. C., Fenton, J. W., II, Maraganore, J. M., Olson, S. T., & Shafer, J. A. (1990) *J. Biol. Chem. 265*, 13484–13489.

Ryckaert, J., Ciccotti, G., & Berendsen, H. J. C. (1977) *J. Comput. Phys. 23*, 327–341.

Rydel, T. J., Ravichandran, K. G., Tulinsky, A., Bode, W., Huber, R., Roitsch, C., & Fenton, J. W., II (1990) *Science 249*, 277–280.

Rydel, T. J., Tulinsky, A., Bode, W., & Huber, R. (1991) *J. Mol. Biol. 221*, 583–601.

Skrzypczak-Jankun, E., Carperos, V. E., Ravichandran, K. G., Tulinsky, A., Westbrook, M., & Maraganore, J. M. (1991) *J. Mol. Biol. 221*, 1379–1393.

Stone, S. R., & Hofsteenge, J. (1986) *Biochemistry 25*, 4622–4628.

Stürzebecher, J. (1984) in *The Thrombin* (Machovich, R., Ed.) pp 131–160, CRC Press, Boca Raton, FL.

Szewczuk, Z., Yue, S.-Y., & Konishi, Y. (1992a) *Peptides: Chemistry and Biology. Proceedings of the 12th American Peptide Symposium* (Smith, J. A., & Rivier, J. E., Eds.) pp 806–807, ESCOM Science Publishers B. V., Leiden, The Netherlands.

Szewczuk, Z., Gibbs, B. F., Yue, S.-Y., Purisima, E. O., & Konishi, Y. (1992b) *Biochemistry 31*, 9132–9140.

Topol, E. J. (1989) *Semin. Hematol. 26*, 25–31.

Verstraete, M. (1990) *Circulation 82* Suppl. No. II, 96–109.

Verstraete, M., Bernard, R., Bory, M., Brower, R. W., Collen, D., De Bono, D. P., Erbel, R., Huhmann, W., Lennane, R. J., Lubsen, J., Mathey, D., Meyer, J., Michels, H. R., Rutsch, W., Schartl, M., Schmidt, W., Uebis, R., & von Essen, R. (1985) *Lancet 1*, 842–847.

Weitz, J. I., Hudoba, M., Massel, D., Maraganore, J., & Hirsh, J. (1990) *J. Clin. Invest. 86*, 385–391.

While, H. D., Rivers, J. T., Maslowski, A. H., Ormiston, J. A., Takayama, M., Hart, H. H., Sharpe, D. N., & Whitlock, R. M. L. (1989) *New Engl. J. Med. 320*, 817–821.

Wilcox, R. G., von der Lippe, G., Olsson, C. G., Jensen, G., Skene, A. M., & Hampton, J. R. (1988) *Lancet 2*, 525–530.

Witting, J. I., Bourdon, P., Brezniak, D. V., Maraganore, J. M., & Fenton, J. W., II (1992) *Biochem. J. 283*, 737–743.

Yue, S.-Y., DiMaio, J., Szewczuk, Z., Purisima, E. O., Ni, F., & Konishi, Y. (1992) *Protein Eng. 5*, 77–85.